Available online at www.sciencedirect.com

SciVerse ScienceDirect

Ceramics International 39 (2013) 1385–1391

CERAMICS INTERNATIONAL

www.elsevier.com/locate/ceramint

Preparation and phosphorus recovery performance of porous calcium–silicate–hydrate

Wei Guan, Fangying Ji*, Qingkong Chen, Peng Yan, Qian Zhang

Key Laboratory of Three Gorges Reservoir Region's Eco-Environment, Ministry of Education, Chongqing University, Chongqing 400045, PR China

Received 18 June 2012; received in revised form 17 July 2012; accepted 24 July 2012
Available online 1 August 2012

Abstract

Porous calcium–silicate–hydrate was synthesized and used to recover phosphorus from wastewater. The principal objective of this study was to explore the phosphorus recovery performance of porous calcium–silicate–hydrate prepared by different Ca/Si molar ratios. Phosphorus recovery mechanism was also investigated via Field Emission Scanning Electron Microscopy (FESEM), Energy Dispersive Spectrum (EDS), Brunauer–Emmett–Teller (BET) and X-ray Diffraction (XRD). The law of Ca^{2+} release was the key of phosphorus recovery performance. Different Ca/Si molar ratios resulted in the changes of pore structures. The increase of specific surface area and the increase in concentration of Ca^{2+} release were well agreement together. The Ca/Si molar ratio of 1.6 for porous calcium–silicate–hydrate is more proper to recover phosphorus. The pore structure of porous calcium–silicate–hydrate provided a local condition to maintain a high concentration of Ca^{2+} release. Porous calcium–silicate–hydrate could release a proper concentration of Ca^{2+} and OH^- to maintain the pH values at 8.5–9.5. This condition was beneficial to the formation of hydroxyapatite. Phosphorus content of porous calcium–silicate–hydrate reached 18.64% after phosphorus recovery.

Keywords: Calcium–silicate–hydrate; Phosphorus recovery; Porous structure; Preparation

1. Introduction

Phosphorus not only plays an important role in water eutrophication, but also is a non-renewable and irreplaceable resource [1]. Global phosphate rock resources will be completely exhausted in 100 years. Therefore recovery from wastewater has been considered as the only way for developing sustainable phosphorus resource [2,3]. Phosphorus recovery from wastewater in the form of hydroxyapatite is a common and simple method [4–6]. However, in the formation process of hydroxyapatite, super-saturation is a common phenomenon. The optimal pH value for the formation of hydroxyapatite is in the range of 10.5–12.5 [7]. This pH value is too high to biochemical treatment system where the pH value is located between 6.0 and 9.0 [8]. For the phosphorus removal by biological treatment process assisted with chemical method, high-pH condition made the two processes difficult to coordinate. Higher pH value also increased significant competition between carbonate and calcium [9]. Meanwhile, the cost of chemical treatment increased and the effective phosphorus composition of the final products are decreased [10].

Calcium–silicate–hydrate (CSH) as seed crystal could be used to remove phosphorus from wastewater through crystallization of hydroxyapatite [11]. Ca^{2+} and OH^- were released from CSH and reacted with the phosphate to form hydroxyapatite under the condition of pH = 8.5–9.5. However, phosphorus content of CSH was too low to recover phosphorus in practical application [12,13]. The efficiency of Ca^{2+} and OH^- release was related to the pore structure of CSH [14] and affected phosphorus recovery performance [15,16]. Ca/Si molar ratio has a significant effect on the pore structure of CSH [17–19]. In the part of phosphorus recovery performance, systematic relationship between Ca/Si molar ratio and phosphorus recovery performance has not been established. The mechanism of the influence of Ca/Si molar ratio on phosphorus recovery performance and the law of Ca^{2+} and OH^- release were still unclear. So it was challenge to

*Corresponding author. Tel./fax: +86 023 65127537.
E-mail address: jfy@cqu.edu.cn (F. Ji).

0272-8842/$ - see front matter © 2012 Elsevier Ltd and Techna Group S.r.l. All rights reserved.
http://dx.doi.org/10.1016/j.ceramint.2012.07.079

determine a proper Ca/Si molar ratio for CSH to recover phosphorus.

The main aim of the research is to find a proper Ca/Si molar ratio for CSH to recover phosphorus. The originality and importance of this paper are highlighted by the following three points:

(1) Porous calcium–silicate–hydrate was synthesized by carbide residue and white carbon black with a dynamic hydrothermal method [20,21]. The influence of Ca/Si molar ratio on phosphorus recovery performance was investigated.
(2) The relationship between pore structure and the law of Ca^{2+} and OH^- release was established by the Avrami kinetic model.
(3) Phosphorus recovery mechanism was studied by FESEM, EDS, BET and XRD on the basis of an in-depth critical investigation.

2. Materials and methods

2.1. Preparation of porous calcium–silicate–hydrate

Porous calcium–silicate–hydrate was synthesized with carbide residue (providing Ca) and white carbon black (providing Si). Carbide residue (calcareous, hoar and powdery) was obtained from Chongqing Changshou Chemical Co. Ltd. and calcined at 700 °C for 2 h. White carbon black (Particles present spherical with homogeneous diameter) was purchased from Chongqing Jianfeng chemical Co. Ltd. Chemical constituents of carbide residue and white carbon black are shown in Table 1. Tobermorite (formula $Ca_5Si_6O_{16}(OH)_2 \cdot 7H_2O$; Theoretical Ca/Si molar ratio of 0.83), a kind of calcium–silicate–hydrate, was purchased from Hdlapp and Ratus (Shanghai) Co. Ltd. The phosphorus solution was adjusted by adding KH_2PO_4 (Analytical reagent, Chongqing Boyi chemical reagent Co. Ltd.) to prepare solution with initial phosphorus concentration of 100 mg/L. The above materials and chemicals were placed into sealed bottles for storage.

Carbide residue and white carbon black were mixed, and the Ca/Si molar ratios were controlled at 0.6, 1.0, 1.6 and 2.2. The mixture was then added to prepared slurries. The slurry was hydrothermally reacted at 170 °C for 6 h and taken out when the temperature was reduced to the natural condition. The hydrothermal reaction was carried out with a liquid/solid ratio of 30. The obtained products were dried at 105 °C for 2 h, and then were ground through a sieve of 200 meshes. The prepared samples with Ca/Si molar ratios of 0.6, 1.0, 1.6 and 2.2 were denoted as CSH: Ca/Si=0.6, CSH: Ca/Si=1.0, CSH: Ca/Si=1.6 and CSH: Ca/Si=2.2, respectively.

2.2. Evaluation of phosphorus recovery performance

Synthetic solution (1 L) was added to bottles, respectively. Certain quality of samples (500, 1000, 2000, 3000, 4000, 5000 and 6000 mg) were added to these bottles respectively and shaken at 40 r/min under controlled temperature conditions (20 °C). Phosphorus concentration of supernatant was measured according to the molybdenum–blue ascorbic acid method (The relative error of data is 0.3%) with a Unico spectrophotometer (UV-2102PCS, Shanghai Unico Instruments Co., Ltd., China) [22]. The solid samples after reaction were then separated from the removed synthetic solution, and were added again to synthetic solution with initial phosphorus concentration of 100 mg/L. This experiment was repeated for several times until the phosphorous concentration was kept unchanged with the addition of samples. Finally, the produced sediments were separated from removed synthetic solution, dried and weighted. Phosphorus contents of samples after phosphorus recovery (P) were calculated by Eq. (1), where C_t is the restrained phosphorus concentration in synthetic solution (mg/L), v is the volume of the solution (L), w is the mass of produced sediment after phosphorus recovery (mg) and C_0 is the initial phosphorus concentration (mg/L).

$$P = \frac{(c_0 - c_t)v}{w} 100\% \quad (1)$$

4 g of samples (CSH: Ca/Si=0.6, CSH: Ca/Si=1.0, CSH: Ca/Si=1.6, CSH: Ca/Si=2.2 and tobermorite) were immersed in 1 L of deionised water respectively contained in a glass bottle, generating samples with a solution concentration of 4 g/L. The bottle was placed on an agitation table and shaken at 40 r/min under controlled temperature conditions (20 °C). Samples of solution were taken after 5, 10, 15, 20, 40, 60, 80 and 100 min of agitation. Ca^{2+} concentration of the samples was determined by EDTA titration (The relative error of data is 0.05%) [23].

Table 1
Chemical components of carbide residue and white carbon black.

	Chemical Components (Contents)/%									
	CaO	SiO_2	Al_2O_3	SO_2	MgO	Fe_2O_3	SrO	NaOH	CuO	H_2O
carbide residue	79.34	3.57	2.14	1.22	0.62	0.21	0.26	–	–	12.64
white carbon black	0.08	97.46	0.16	1.82	–	0.03	–	0.29	0.02	0.14

2.3. Characterization methods

XRD patterns were collected in a XD-2 instrument (Persee, China) using Cu Kα radiation. FESEM images were collected on an S-4800 field emission scanning electron microscope (Hitachi, Japan). BET surface areas were measured by nitrogen adsorption at 77.35 K on an ASAP-2010 adsorption apparatus (Micromeritics, USA).

3. Results and discussion

3.1. Phosphorus recovery performance of porous calcium–silicate–hydrate

The influence of reaction time on restrained phosphorus concentration is shown in Fig. 1. A sharp decrease in phosphorus concentration was observed during the first 20 min. phosphorus concentration declined slightly with prolonged time. The difference of the restrained phosphorus concentration was significant when the reaction reached equilibrium at 60 min. Restrained phosphorus concentration reached 22.19 mg/L when the molar ratio of Ca/Si was 0.6. With the increase in Ca/Si molar ratio, phosphorus removal capacity of samples is improved significantly. Restrained phosphorus concentration was 2.16 mg/L when the molar ratio of Ca/Si was 2.2.

Fig. 2 shows the removal of phosphorus with different samples dosing. Efficiency of phosphorus removal was improved when the dosage increased and the highest removal efficiency was obtained at 4000 mg/L. Then, the phosphorus removal efficiency almost remained stable with the further increase in samples dosing. Comparatively speaking, CSH: Ca/Si=2.2 showed the highest phosphorus removal efficiency. Restrained phosphorus concentration was only 2.16 mg/L and the mass of sediment was 3750 mg. However, the phosphorus content of CSH: Ca/Si=2.2 was only 2.6%. Phosphorus content of samples could be enhanced due to circulation of phosphorus removal.

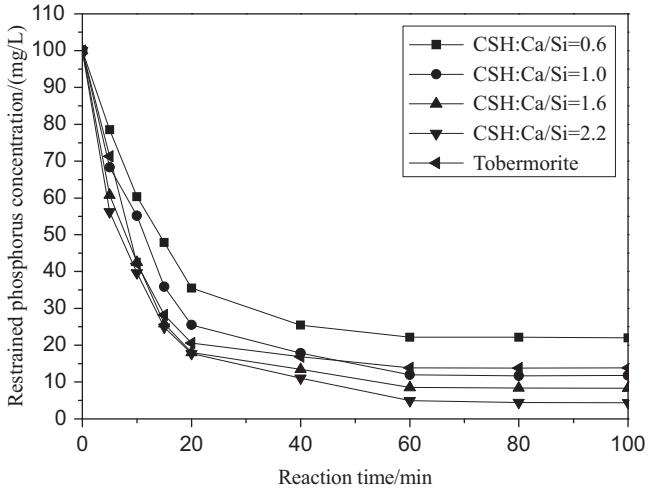

Fig. 1. Influence of reaction time on restrained phosphorus concentration.

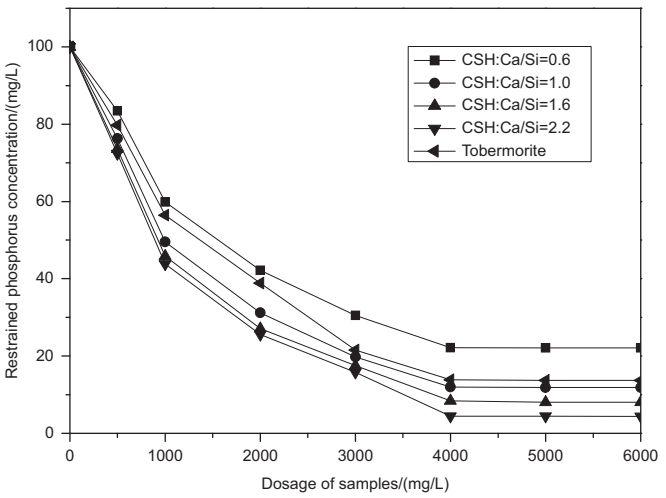

Fig. 2. Influence of samples dosage on restrained phosphorus concentration.

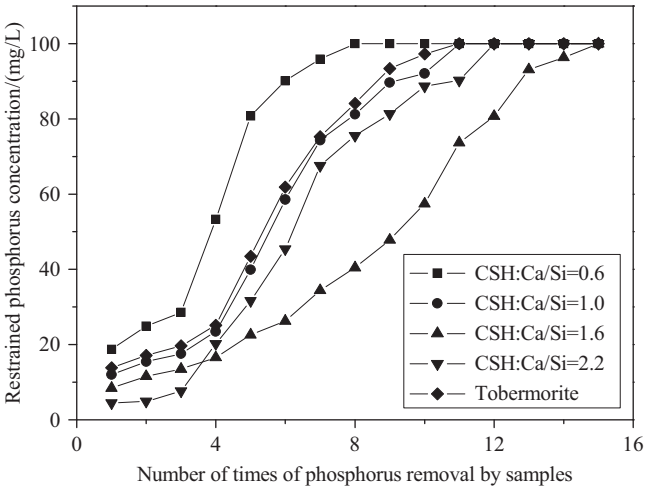

Fig. 3. Changes of restrained phosphorus concentration by circulation of phosphorus removal.

Samples were separated from the synthetic solution removed, and then added to synthetic solution with initial phosphorus concentration 100 mg/L. Changes of restrained phosphorus concentration are shown in Fig. 3. Phosphorus removal performance of CSH: Ca/Si=2.2 maintained well during first 3 times, and ceased after the 12th time. Phosphorus content of CSH: Ca/Si=2.2 was 14.10%, while phosphorus content of CSH: Ca/Si=1.6 reached 18.64%. CSH: Ca/Si=1.6 had a higher phosphorus recovery performance compared with CSH: Ca/Si=2.2. Phosphorus removal performance of samples was related to pH values. With the times of phosphorus removal prolonged, pH values decreased (Fig. 4). As seen, CSH: Ca/Si=2.2 contributed to a range of high pH values (pH=9.8–10.2) at first 3 times, and declined sharply at the 4th time (pH=8.5). CSH: Ca/Si=1.6 could maintain high pH values (pH=8.5–9.5) for a long time (10 times of

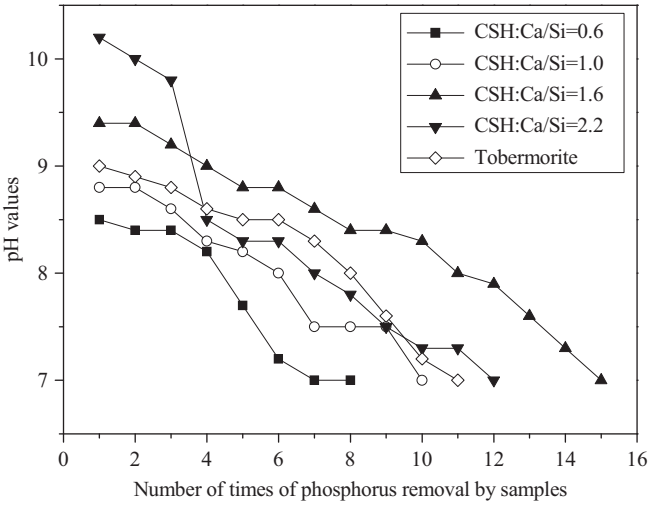

Fig. 4. Changes of pH values by circulation of phosphorus removal.

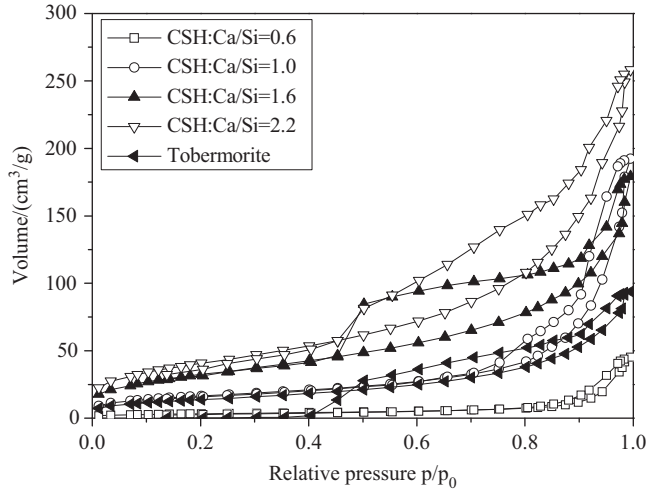

Fig. 5. Nitrogen adsorption–desorption isotherms on samples.

phosphorus removal). This condition was beneficial to circulation of phosphorus removal.

3.2. The pore structure of porous calcium–silicate–hydrate

Nitrogen adsorption–desorption isotherms on samples are shown in Fig. 5. The results suggested the phenomenon of adsorption hysteresis loop. That means mesopore or narrow gap pore existed on samples [24]. Adsorption in mespore occurred mainly in medium pressure region ($0.4 < p/p_0 < 0.9$). With the increase in Ca/Si molar ratio, the phenomenon of adsorption hysteresis loop became obvious and the adsorption curve increased. Specific surface areas of CSH: Ca/Si=0.6, CSH: Ca/Si=1.0, CSH: Ca/Si=1.6, CSH: Ca/Si=2.2 and tobermorite were 11.91, 59.67, 113.36, 121.03 and 49.85 m^2/g, respectively. Pore volumes of these samples were 0.07, 0.30, 0.52, 0.65 and 0.15 cm^3/g, correspondingly. The increase of Ca/Si molar ratio resulted in smaller pore size, larger specific surface area and pore volume.

The surface structure of tobermorite, CSH: Ca/Si=1.6 and CSH: Ca/Si=2.2 was examined by FESEM observations and EDS analyses (Fig. 6). Compared with tobermorite, CSH: Ca/Si=1.6 had an obverse fibrous-network structure with a large number of mesopores. CSH: Ca/Si=2.2 had massive flake crystal besides fibrous-network structure. EDS analyses confirmed that the coarse surface of tobermorite, CSH: Ca/Si=1.6 and CSH: Ca/Si=2.2 consisted predominantly of Ca and Si. Ca/Si molar ratio was 0.8, 1.5 and 2.0, respectively. Ca/Si molar ratio of materials decreased after synthesis due to the loss of partial Ca^{2+} when filtering slurry. Thus, the single phosphorus removal efficiency of CSH increased with the increased specific surface area.

3.3. Kinetics of Ca^{2+} release

The experiments showed that Ca^{2+} concentrations increased with the increase of Ca/Si molar ratio (Fig. 7). Concentrations of Ca^{2+} released from tobermorite, CSH: Ca/Si=1.6 and CSH: Ca/Si=2.2 were 2.10, 3.56, 4.91 mg/g, respectively. The experimental capacities of Ca^{2+} release were plotted according to Avrami kinetic model equation (Eq. (2)) [25].

$$-\ln(1-x) = kt^n \quad (2)$$

where k is the kinetic constant, n is the characteristic constant of solid, t is the reaction time (min) and x ($x = C_t/C_{max}$, C_t is concentration of time t (mg/L) and C_{max} is concentration of the maximum (mg/L)) is the fraction conversion. The characteristic constant n was 0.9019. The kinetic constants were determined by fitting the Avrami kinetic model to the experimental data obtained from Fig. 6 (Table 2). The high correlation coefficients ($R^2 > 0.99$) indicated that this model could describe the law of Ca^{2+} release well.

As shown in Table 2, k became larger with increasing Ca/Si molar ratio. Combined with specific surface area (S) of materials, a relationship between k and S could be established (Eq. (3)).

$$k = 0.022S^{0.292} \quad R^2 = 0.9135 \quad (3)$$

According to Eq. (3), specific surface area of samples and the rate of Ca^{2+} release were in good agreement with each other. The relationship between specific surface area and dissolved concentration of Ca^{2+} was obtained by substituting Eq. (3) into Eq. (2).

$$-\ln(1-x) = 0.022S^{0.292}t^{0.9019} \quad (4)$$

According to Eq. (4), concentration of Ca^{2+} release was related to specific surface area. This result demonstrated the influence of Ca/Si molar ratio on phosphorus recovery capacity. Ca/Si molar ratio affected the pore structure and the capacity of Ca^{2+} release. Ca^{2+} was released faster due to larger specific surface area. Porous structure provided a

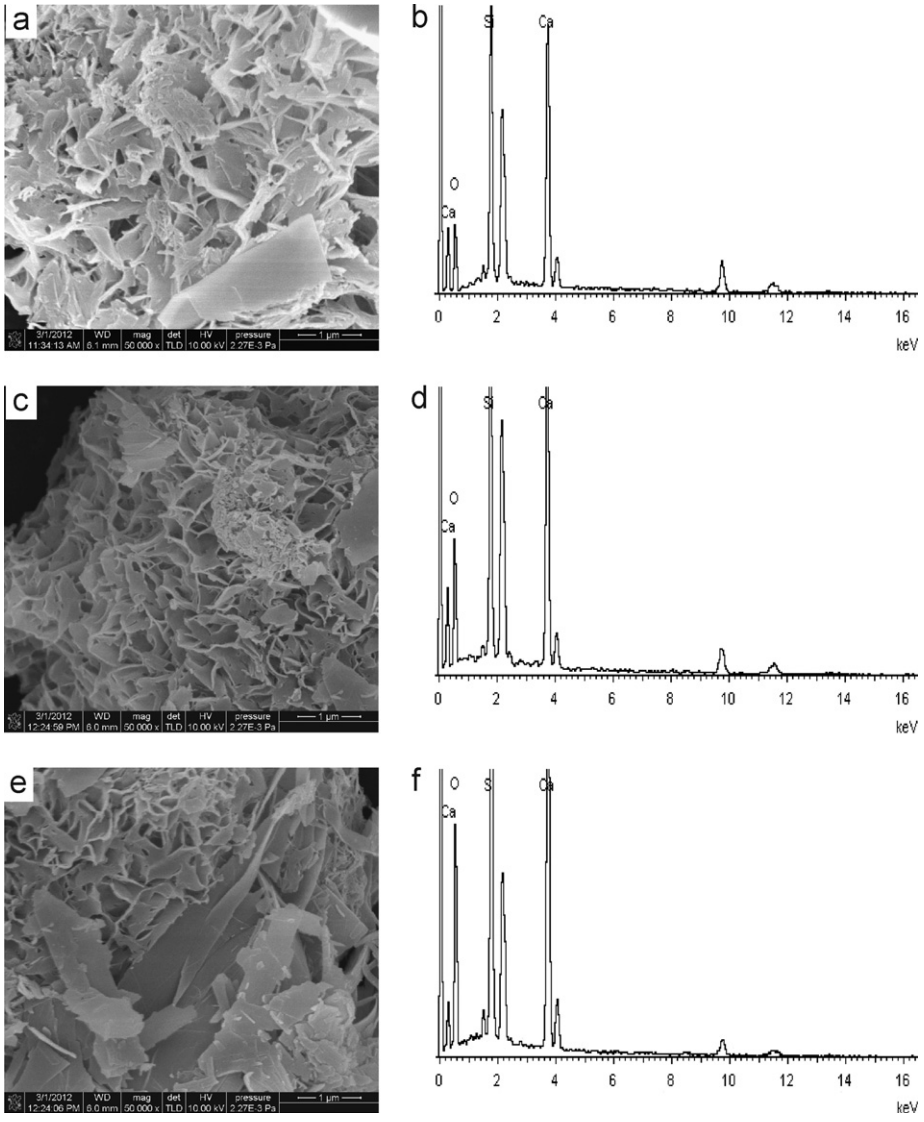

Fig. 6. FESEM observations and EDS analyses. (a) surface of tobermorite; (b) chemical analysis of tobermorite; (c) surface of CSH: Ca/Si=1.6; (d) chemical analysis of CSH: Ca/Si=1.6; (e) surface of CSH: Ca/Si=2.2; and (f): chemical analysis of CSH: Ca/Si=2.2.

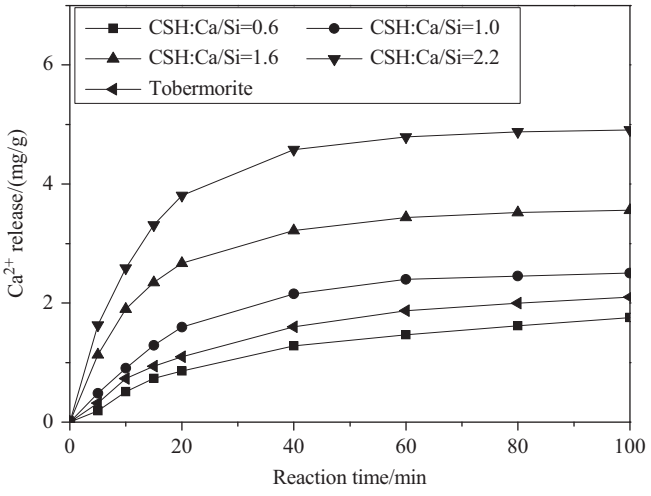

Fig. 7. Concentrations of Ca^{2+} released from samples.

Table 2
Correlation equations and rate constants for the Avrami kinetic model describing Ca^{2+} release.

Samples	Correlation equation	k	R^2
CSH: Ca/Si=0.6	$-\ln(1-x)=0.0472t^{0.9019}$	0.0472	0.9955
Tobermorite	$-\ln(1-x)=0.0604t^{0.9019}$	0.0604	0.9943
CSH: Ca/Si=1.0	$-\ln(1-x)=0.0741t^{0.9019}$	0.0741	0.9933
CSH: Ca/Si=1.6	$-\ln(1-x)=0.0866t^{0.9019}$	0.0866	0.9980
CSH: Ca/Si=2.2	$-\ln(1-x)=0.0966t^{0.9019}$	0.0966	0.9991

local condition to maintain a high concentration of Ca^{2+} release. Compared CSH: Ca/Si=1.6 with CSH: Ca/Si=2.2, the former had higher phosphorus recovery performance in fact. So the law of Ca^{2+} release is the key of phosphorus recovery performance. CSH: Ca/Si=1.6 could release a suitable concentration of Ca^{2+} and OH^- to

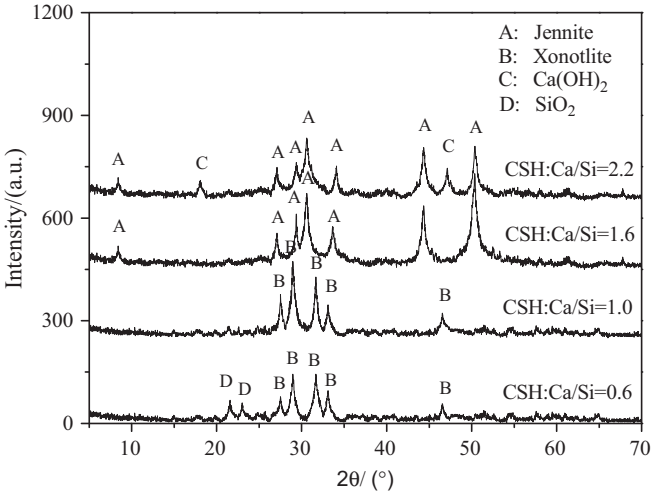

Fig. 8. X-ray diffraction (XRD) patterns of samples.

maintain the pH values during 8.5–9.5. Phosphate existed in the form of HPO_4^{2-} in the range of these pH values [26]. Ca^{2+}, OH^- and HPO_4^{2-} formed a local condition with high concentration. This condition was beneficial to the formation of hydroxyapatite with pH = 8.5–9.5.

The mechanism could be further investigated by XRD. The XRD patterns of samples were compared (Fig. 8). The production was xonotlite (PDF card 23-0125, chemical formula $Ca_6Si_6O_{17}(OH)_2$) when Ca/Si molar ratio was 0.6:1 and 1:1. For CSH: Ca/Si = 0.6, principal peaks of SiO_2 were emerged at 20.305° and 21.562°. The principal peaks in CSH: Ca/Si = 1.6 and CSH: Ca/Si = 2.2 were assigned to jennite (PDF card 18-1206; formula $Ca_9Si_6O_{18}(OH)_6 \cdot 8\,H_2O$; theoretical Ca/Si molar ratio of 1.5). The XRD pattern of CSH: Ca/Si = 2.2 showed the existence of $Ca(OH)_2$. The coverage of the formed $Ca(OH)_2$ was in good accordance with the result based on FESEM observations [27].

The experiments indicated that jennite has the stronger capacity of Ca^{2+} release compared with xonotlite and tobermorite. Low Ca/Si molar ratio resulted in the surplus of white carbon black. Therefore, a Si enriched layer was formed on the material's surface and blocked Ca^{2+} release. Subsequently, phosphorus recovery capacity of material decreased. The formation of $Ca(OH)_2$ was due to the surplus of carbide residue with high Ca/Si molar ratio. The single phosphorus removal efficiency of CSH: Ca/Si = 2.2 was better than other samples due to the existence of $Ca(OH)_2$. Nevertheless, massive Ca^{2+} was released and reacted with phosphate ion as quickly as the material immersed in synthetic solution. Hydroxyapatite layer formed in a short time and led to obstruction of pore structure. So the capacity of Ca^{2+} release decreased.

4. Conclusions

Porous calcium–silicate–hydrate was synthesized by carbide residue and white carbon black with a dynamic hydrothermal method. Ca/Si molar ratio exerted significant influence on phosphorus recovery performance of porous calcium–silicate–hydrate. The Ca/Si molar ratio of 1.6 for porous calcium–silicate–hydrate is more proper to recover phosphorus. Porous calcium–silicate–hydrate could recover phosphorus with phosphorus content of 18.64%.

The law of Ca^{2+} and OH^- release was the key of phosphorus recovery efficiency. Changes of Ca/Si molar ratio led to the different pore structure. The increase of specific surface area and the increase in concentration of Ca^{2+} release were in good agreement with each other.

Further analysis by XRD indicated that two situations affected the law of Ca^{2+} release. On the one hand, low Ca/Si molar ratio led to the formation of Si enriched layer. On the other hand, $Ca(OH)_2$ formed due to high Ca/Si molar ratio.

References

[1] K. Suzkui, Y. Tanaka, K. Kuioda, K. Kuroda, D. Hanajima, Y. Fukumoto, T. kasuda, M. Waki, Removal and recovery of phosphorous from swine wastewater by demonstration crystallization reactor and struvite accumulation device, Bioresource Technology 8 (2007) 1573–1578.

[2] Y.L. Yang, X. Li, C.X. Guo, F.W. Zhao, F. Jia, Efficiency and mechanism of phosphorus removal by coagulation of iron–manganese composited oxide, Chemical Research in Chinese Universities 2 (2009) 224–227.

[3] Y.H. Song, D. Donnert, U. Berg, G.W. Peter, R. Nueesch, Seed selections for crystallization of calcium phosphate for phosphorus recovery, Journal of Environmental Science 19 (2007) 591–595.

[4] X.C. Chen, H.N. Kong, D.Y. Wu, X.Z. Wang, Y.Y. Lin, Phosphate removal and recovery through crystallization of hydroxyapatite using xonotlite as seed crystal, Journal of Environmental Science 21 (2009) 575–580.

[5] V.M. Elisabeth, K. Barr, Controlled struvite crystallisation for removing phosphorus from anaerobic digester sidestreams, Journal of Water Resources 1 (2001) 151–159.

[6] Y.H. Song, G.W. Peter, U. Berg, R. Nueesch, D. Donnert, Calcite-seed crystallization of calcium phosphate for phosphorus recovery, Chemosphere 63 (2006) 236–243.

[7] J.B. Liu, X.Y. Ye, H. Wang, M.K. Zhu, B. Wang, H. Yan, The influence of pH and temperature on the morphology of hydroxyapatite synthesized by hydrothermal method, Ceramics International 29 (2003) 629–633.

[8] C.R. Hood, A.A. Randall, A biochemical hypothesis explaining the response of enhanced biological phosphorus removal biomass to organic substrates, Water Research 11 (2011) 2758–2766.

[9] P. Battistoni, P. Pavan, M. Prisciandaro, F. Cecchi, Struvite crystallization: a feasible and reliable way to fix phosphorus in anaerobic supernatants, Water Research 11 (2000) 3033–3041.

[10] S. Sengupta, A. Pandit, Selective removal of phosphorus from wastewater combined with its recovery as a solid-phase fertilizer, Water Research 45 (2011) 3318–3330.

[11] P. Battistoni, A. Dangelis, P. Pavan, M. Prisciandaro, F. Cecchi, Phosphorus removal from a real anaerobic supernatant by struvite crystallization, Water Research 9 (2001) 2167–2178.

[12] A. Renman, G. Renman, Long-term phosphate removal by the calcium–silicate material Polonite in wastewater filtration systems, Chemosphere 79 (2010) 659–664.

[13] L.E. de-Bashan, Y. Bashan, Recent advances in removing phosphorus from wastewater and its future use as fertilizer (1997–2003), Water Research 38 (2004) 4222–4246.

[14] H.B. Yin, Y. Yun, Y.L. Zhang, C.X. Fan, Phosphate removal from wastewaters by a naturally occurring, calcium-rich sepiolite, Journal of Hazardous Materials 198 (2011) 362–369.

[15] L.J. Westholm, Substrates for phosphorus removal—potential benefits for on-site wastewater treatment?, Water Research 40 (2006) 23–36

[16] L. Baur, K. Peter, D. Mavrocordatos, B. Wehrli, C.A. Johnson, Dissolution–precipitation behaviour of ettringite, monosulfate, and calcium silicate hydrate, Cement and Concrete Research 34 (2004) 341–348.

[17] J.C. Jeffrey, J.J. Thomas, Hal F.W. Taylor, H.M. Jennings, Solubility and structure of calcium silicate hydrate, Cement and Concrete Research 34 (2004) 1499–1519.

[18] S.U. Sezen, Sejung S.R. Chae, C.J. Benmore, H.R. Wenk, Compositional evolution of calcium silicate hydrate(C–S–H) structures by total X-ray scattering, Journal of the American Ceramic Society 2 (2012) 793–798.

[19] I.G. Richardson, Tobermorite/jennite-and tobermorite/calcium hydroxide-based models for the structure of C–S–H: applicability to hardened pastes of tricalcium silicate, β-dicalcium silicate, Portland cement, and blends of Portland cement with blast-furnace slag, metakaolin, or silica fume, Cement and Concrete Research 34 (2004) 1733–1777.

[20] M.Q. Li, H.X. Liang, Formation of micro-porous spherical particles of calcium silicate (xonotlite) in dynamic hydrothermal process, China Particuology 3 (2004) 124–127.

[21] A.A.P. Mansur, H.S. Mansur, Preparation, characterization and cytocompatibility of bioactive coatings on porous calcium–silicate–hydrate scaffolds, Materials Science and Engineering C 30 (2010) 288–294.

[22] J.P. Gustafsson, A. Renman, G. Renman, K. Poll, Phosphate removal by mineral-based sorbents used in filters for small-scale wastewater treatment, Water Research 42 (2008) 189–197.

[23] J. Kim, C. Vipulanandan, Effect of pH, sulfate and sodium on the EDTA titration of calcium, Cement and Concrete Research 33 (2003) 621–627.

[24] W.S. Zhang, H.X. Wang, J.Y. Ye, Pore structure and surface fractal characteristics of calcium silicate hydrates contained organic macromolecule, Journal of the Chinese Ceramic Society 12 (2006) 1497–1502 (in Chinese).

[25] N. Demirkiran, A. Kunkul, Dissolution kinetics of ulexite in perchloric acid solutions, International Journal of Mineral Processing 83 (2007) 76–80.

[26] Y. Liu, X. Sheng, Y.H. Dong, Y.J. Ma, Removal of high-concentration phosphate by calcite: effect of sulfate and pH, Desalination 289 (2012) 66–71.

[27] E. Gallucci, K. Scrivener, Crystallization of calcium hydroxide in early age model and ordinary cementitious systems, Cement and Concrete Research 37 (2007) 492–501.